Journal of *Marine Science and Engineering*

MDPI

Article

A Dynamic Cloud Center of Gravity Model for Real-Time System-Level Health Status Assessment of Intelligent Ship

Lei Guo [1,2], Tianjian Wang [1,2], Xiao Dong [1,2], Peng Zhang [1,3], Hong Zeng [1,2,3] and Jundong Zhang [1,2,3,*]

[1] Marine Engineering College, Dalian Maritime University, Dalian 116026, China; engineering_glay@dlmu.edu.cn (L.G.)
[2] Liaoning Marine Simulation and Monitoring Research Center, Dalian Maritime University, Dalian 116026, China
[3] Collaborative Innovation Research Institute of Autonomous Ship, Dalian Maritime University, Dalian 116026, China
* Correspondence: zhjundong@dlmu.edu.cn

Abstract: To enable early identification of failure risks in ship systems and equipment, a dynamic cloud center of gravity model is developed for real-time system-level health assessment. First, the Functional Analysis System Technique (FAST) was applied to decompose the operational functions and dependencies of the intelligent machinery room system, enabling the structured establishment of a hierarchical evaluation index system. The comprehensive weight is derived through synergistic application of the fuzzy set (FS) theory and entropy weight. This process integrated expert-defined functional boundaries with measurable parameters critical to system performance. Then, an improved cloud center of gravity method based on the Gaussian cloud model and sliding time window method is used for the system's adaptive health value calculation. The dynamic health model can achieve continuous online assessment and track the further evolution of the system. Finally, the proposed model is applied to the Fuel Oil Supply System (FOSS). The integration of system performance output and disassembly inspection results demonstrates that the method proposed in the article more accurately reflects the true health status changes in the system when mapping health values.

Keywords: intelligent ship; cloud barycenter; condition assessment; health model; reliability; ship systems

check for updates

Academic Editor: Hsuan-Shih Lee

Received: 23 January 2025
Revised: 13 February 2025
Accepted: 16 February 2025
Published: 19 February 2025

Citation: Guo, L.; Wang, T.; Dong, X.; Zhang, P.; Zeng, H.; Zhang, J. A Dynamic Cloud Center of Gravity Model for Real-Time System-Level Health Status Assessment of Intelligent Ship. *J. Mar. Sci. Eng.* **2025**, *13*, 384. https://doi.org/10.3390/jmse13020384

Copyright: © 2025 by the authors. Licensee MDPI, Basel, Switzerland. This article is an open access article distributed under the terms and conditions of the Creative Commons Attribution (CC BY) license (https://creativecommons.org/licenses/by/4.0/).

1. Introduction

With advancements in information technology and artificial intelligence, Intelligent Ship Systems (ISSs) are achieving greater autonomy, thereby requiring fewer crew members onboard. This enhanced autonomy effectively reduces accidents attributable to human factors [1]. In order to realize the unmanned management of a system, it is very important to know the state of the system at any time. A reliable dynamic model is essential for evaluating the health conditions of mechanical systems and equipment, enabling the performance of reasonable maintenance.

A program based on Condition-Based Maintenance (CBM) offers valuable insights to inform maintenance decisions, thereby enhancing the safety, reliability, and maintainability of engineering systems [2–5]. Therefore, system-level real-time condition assessment is becoming more attractive.

Traditional condition monitoring and reliability assessment methods typically either compare operational results under identical working conditions or calculate equipment

reliability using failure data aggregated from multiple identical units [6,7]. New condition monitoring and assessment research has incorporated component interaction analysis through adaptive measurement parameters, enabling targeted identification of faults in interconnected subsystems. This method is applied to the fault pattern recognition of a single device or component such as gearboxes [4], compressors, bearings [8], pumps [9,10], and wind turbines [11,12]. Consequently, when dealing with a state monitoring system that targets a particular component, identifying the origin of a dynamic signature can pose a significant challenge. However, comprehensive condition monitoring systems capable of fusing multi-device operational data enable more granular and reliable diagnostic assessments [13]. The effectiveness of such monitoring critically determines CBM program performance. Building on these observational capabilities, a dynamic CBM framework with adaptive inspection strategies is presented, formulated through Partially Observable Markov Decision Processes (POMDPs) [14].

In recent years, health condition assessment has gained widespread application in various domains, including lithium batteries, aerospace, bridges, power grids, nuclear power, and others [13,15–17]. The state of the system can be described as a collection of random variables that oscillate between factor and variable nodes, characterized by their mean and covariance values. Utilizing Bayesian theory, the assessment of a smart grid's condition is achieved through the iterative processing of information [18]. A robust approach for state estimation, known as the Smooth Variable Structure Filter (SVSF), is employed to mitigate the impact of measurement uncertainty, thereby enhancing the effectiveness of the state assessment model [19]. Utilizing operational signals from the air conditioning system, the health index was derived through data-driven analytics, while system degradation trajectories were probabilistically forecasted via Bayesian inference integrated with dynamic linear modeling [20]. New strategies have been proposed for health assessment of a rolling bearing [8] and a wind turbine [11] on account of multiple characteristic parameters. The enhanced fuzzy synthetic evaluation framework [21] and support vector machine methodology [22] have been effectively implemented for condition monitoring in wind turbine operational assessments.

Current research into a system-level dynamic health assessment and failure prognostics remains underexplored, particularly regarding integrated methodological frameworks and temporal degradation modeling. The interdependencies among component behaviors significantly amplify systemic complexity. Liu et al. [23] and Moghaddass et al. [24], respectively, pioneered methodological frameworks for system-level dynamic reliability assessment and failure prognostics, focusing on degradation trajectory modeling and uncertainty quantification. In the process of system monitoring and adaptive condition assessment, the degradation process of components should be analyzed independently [25]. A structure has been introduced for incorporating condition monitoring and inspection data into the process of dynamic risk assessment [26,27].

In the field of uncertainty modeling and knowledge engineering, probability theory and FS theory have established themselves as fundamental analytical approaches for addressing information ambiguity and incomplete data characterization. Probability theory is primarily used to study random phenomena, and it can effectively handle random uncertainty. Over the years, the concept of fuzzy random reliability, which is used to assess the safety of architectural structures, has attracted increasing interest from researchers due to its advantages in addressing both fuzziness and randomness. Based on the theory of fuzzy random variables, significant advancements in hybrid computational methods have been proposed to address the issues of fuzzy random reliability in various fields, such as coastal engineering, industrial engineering, and so on [28–30]. Consequently, an evaluation method for mission reliability of fuzzy multistate manufacturing systems, utilizing an extended

stochastic flow network, was introduced [31]. Cloud theory systematically integrates the methodological strengths of probabilistic statistics and fuzzy mathematics, establishing a novel synthesis that transcends conventional membership function paradigms while explicitly characterizing the stochastic–fuzzy coupling inherent in complex systems [32,33]. Some researchers have found that this method can provide a cognitive framework to tackle the problem of systems or structures reliability analysis [34,35].

Cloud barycenter evaluation method is a comprehensive evaluation method originated from cloud theory, data mining, and knowledge representation. It can unify the fuzziness and randomness of multiple equipment and multiple parameter systems, and establish the mutual mapping between qualitative language and quantitative value, which provide an effective mathematical method for health assessment. This methodology has been predominantly implemented for condition monitoring assessments of large-scale engineered systems within defense applications [36,37]. The traditional cloud barycenter condition assessment method can only be applied to a limited set of fixed indicators, typically employing fixed weights to yield static evaluation results. With these considerations in mind, a dynamic condition assessment model is proposed to improve the indicators and make it suitable for systems which have multi-type parameters. The principal outcomes of this research are listed as follows:

(1) This work presents an indicator system designed for condition assessment, which is grounded in the FAST method. For unmanned ships, it provides a more accurate representation of the technical status of an ISS.
(2) A dynamic health model for condition assessment is proposed based on an improved cloud barycenter. The health value could be updated with new monitored data, and the continuous health value could be obtained.
(3) A dynamic cloud barycenter model with adaptive sliding window control was developed for system-level health assessment under time-varying conditions. It integrates multi-type indicator normalization (e.g., cost, interval, benefit) and probabilistic–fuzzy uncertainty quantification, overcoming the limitations of static weight allocation in traditional methods.

The remainder of the paper is organized as follows. Section 2 describes the typical characteristics of the ISS and problems in system condition assessment. The proposed dynamic cloud barycenter method is described in Section 3. In addition, the establishment of the assessment indicator system based on the FAST and comprehensive weight is discussed, and the formulation is described. The FOSS was selected as a case study to demonstrate the viability of the method in Section 4. Lastly, Section 5 presents a summary of the conclusions and outlines potential avenues for future research.

2. Problem Description and Framework

2.1. System Characterization and Modeling Premises

ISSs are complex systems including mechanical, electrical, and hydraulic systems. The systems have the characteristics of multiple parameters and multiple types of equipment, which makes health assessment very complex. With the improvement of the system intellectualization, the state perception can be measured from the ordinary parameters to the omni-directional state perception, and the corresponding indicator parameters can always be found to reflect the technical performance. The sufficient state parameters, appropriate data processing methods, and accurate health models are all very essential for the assessment of real-time health conditions.

Before establishing a model for dynamic health assessment, some modeling premises concerning the considered system were presented, as follows:

Premise 1: System Demarcation.

The intelligent systems involved in this research were mainly related to the ship piping systems. The systems consisted of pumps, filters, valves, heat exchangers, pipes, accessories, etc. The functions of these systems were relatively clear, usually in series, parallel, or mixed.

Premise 2: Data Acquisition Protocol.

Routine parameters were selected in the assessment process that could be covered by existing or additional sensors. The parameter collection processes were easier to implement in engineering, and they did not destroy the system structure.

Premise 3: Maritime Operational Context.

In contrast to systems on land, the ship operation characteristics objectively needed the systems and equipment to have higher reliability. As a result, the ISS operated in a relatively stable manner, with minimal changes in state parameters and low fluctuation rates over an extended period. These working conditions and parameter variations facilitated the development of a comprehensive assessment approach.

Premise 4: Degradation Boundary Condition.

In the process of health assessment, in this research, the changes in the health status caused by the degradation, environment, working conditions, maintenance, and so on were considered. The processes after the loss of system functions were not considered.

Premise 5: Technological Baseline.

At present, ship systems realize online monitoring based on parameters. Some systems have achieved static evaluation based on historical parameters, but dynamic health assessment has not been realized. It was necessary to keep abreast of the latest state of the system for CBM and autonomous decision-making.

2.2. Framework

To investigate the real-time condition assessment at the system level, this article presents a dynamic health model, constructs a health indicator, and realizes system health management. Figure 1 demonstrates the framework of system condition assessment. The proposed model was constructed based on the improved cloud barycenter method. The detailed calculation process is as follows:

Step 1: The FAST was chosen to establish an assessment indicator system. Through the analysis of the system's structure and function, appropriate indicator parameters were selected to describe the technical state of the system.

Step 2: System operational parameters were acquired through distributed sensor networks, followed by multivariate signal normalization and noise reduction preprocessing.

Step 3: Indicator weights were determined using the comprehensive weighting approach.

Step 4: A cloud barycenter model, rooted in cloud theory, was developed and refined based on indicator parameter characteristics.

Step 5: Utilizing steps 1–4, a dynamic health model was established.

Step 6: The model was implemented on the chosen system, yielding real-time health values.

Step 7: The health value was used to monitor the health status of the whole system and realized the health management. According to the health value, engineers could make reasonable operation and maintenance decisions.

This study introduces a proposed method aimed at addressing the aforementioned issues and enabling a dynamic reliability assessment of the systems. In the case study section, the widely used ship power system was selected as an example, which was composed of various equipment and components in series.

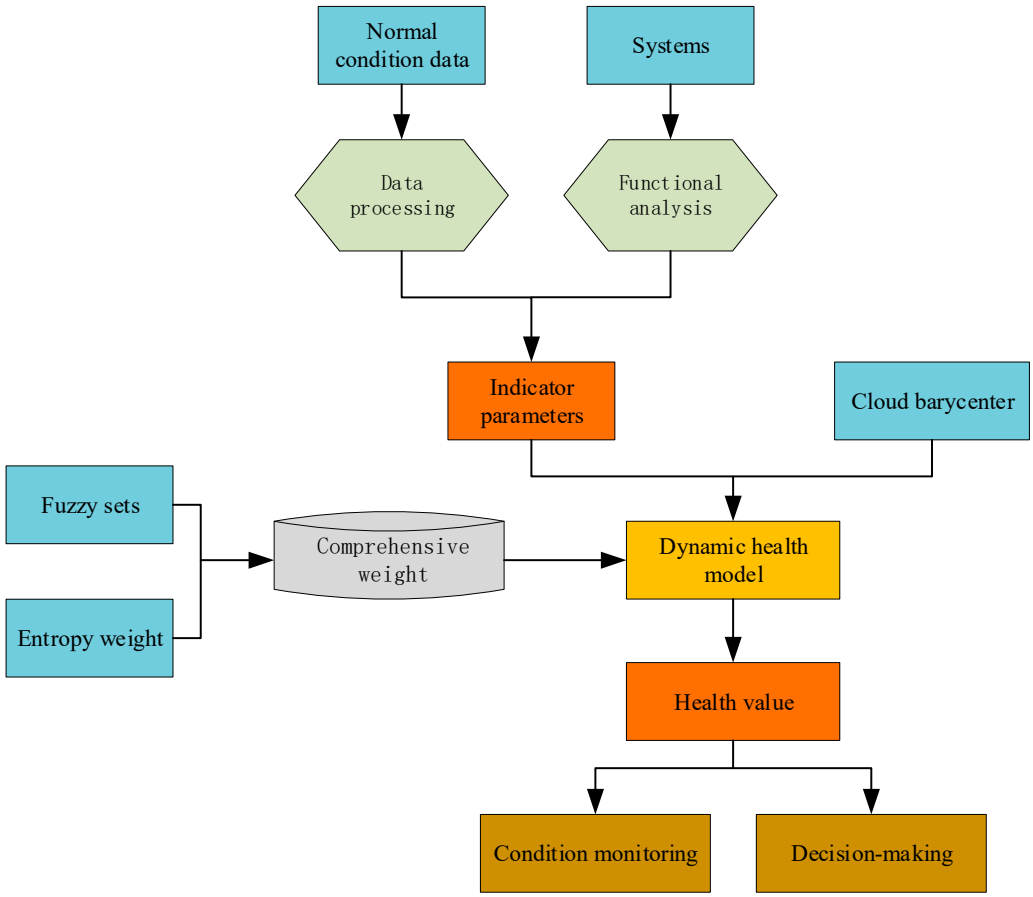


Figure 1. Schematic of system condition assessment.

3. Methodology

3.1. Cloud Barycenter Method

The health value was calculated using the condition assessment method, which measured the deviation degree between the current and ideal states. The deviation was expressed by the cloud barycenter deviation based on cloud theory.

3.1.1. Gaussian Cloud Model

Cloud models can be represented by three numerical characteristics as shown in Figure 2, namely Ex (expectation), En (entropy), and He (hyper entropy) [38]. Ex serves as the quintessential example of a concept, En is employed to determine the granularity level of the concept, and He depicts the degree of uncertainty in the concept's granularity. Cloud transformations, namely Forward Cloud Transformation (FCT), was used to achieve the transformation from the intension to the extension of a concept [39].

FCT algorithm [38].

The inputs to the algorithm include the numerical characteristics (Ex, En, He) and the number of cloud drops n. Cloud drops x_i with certainty degrees $\mu(x_i)$ $(i = 1, 2, \cdots, n)$ is the output.

Step 1: Generate a normally distributed random number y_i with expectation En and variance He, i.e., $y_i = R_N(En,\ He)$.

Step 2: Generate a normally distributed random number x_i with expectation Ex and variance y_i^2, i.e., $x_i = R_N(Ex,\ y_i)$.

Step 3: Calculate certainty degree $\mu(x_i)\ = exp\left\{-\frac{(x_i - Ex)^2}{2y_i^2}\right\}$.

Step 4: x_i with certainty degree $\mu(x_i)$ is a Gaussian cloud drop.

Step 5: Repeat steps 1–4 until n cloud drops are generated.

FCT algorithm illustrate that each cloud drop x_i was generated by two normal random numbers, and y_i was the input to generate x_i. Therefore, n cloud drops x_i were generated by n normal distributions $N(Ex, y_i^2)$ $(i = 1, 2, \ldots, n)$, where in each y_i was generated by the normal distribution $N(En, He)$.

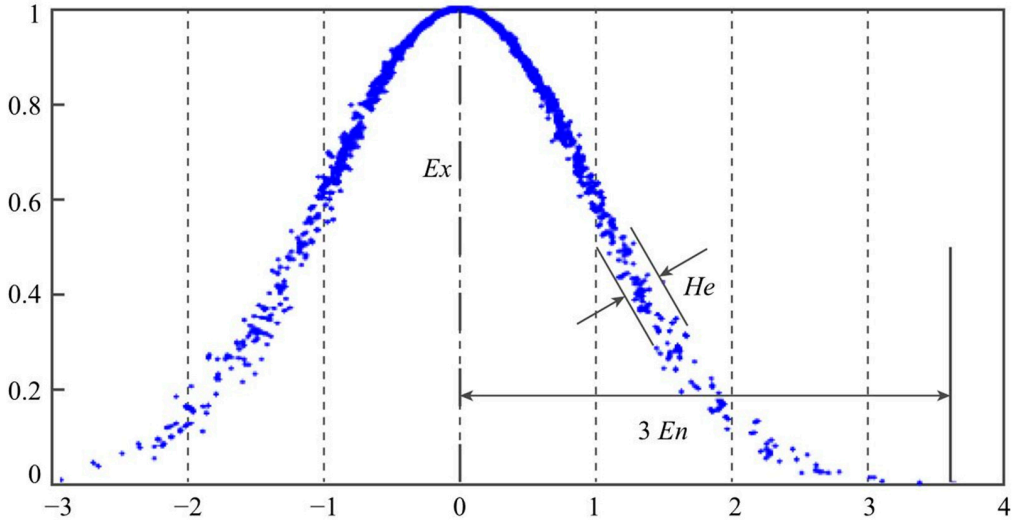


Figure 2. Cloud model and digital characteristic.

3.1.2. Cloud Barycenter

The mathematical expression of the barycenter was as follows:

$$T = a \times b, \tag{1}$$

where a is the position of the barycenter, which is the expectation of the three digital features of the cloud model, and b is the height of the barycenter, which is the corresponding weight.

The specific steps for determining the health status with the cloud barycenter method were as follows:

(1) Extraction of digital features

According to the assessment index system, the digital characteristics of the cloud model corresponding to each index in the data samples m were extracted:

$$Ex = \frac{(x_1 + x_2 + \cdots + x_m)}{m}, \tag{2}$$

$$En = \frac{\max(x_1, x_2, \cdots, x_m) - \min(x_1, x_2, \cdots, x_m)}{6}. \tag{3}$$

(2) Calculation of the deviation degree

A multi-dimensional integrated cloud model composed of various evaluation indicators was used to represent the health status of the system. If the number of the indicators was n, the corresponding integrated cloud barycenter vector G could be expressed as follows:

$$G = (G_1, G_2, \ldots, G_n), \tag{4}$$

where $G_i = a_i \times b_i$, $b_i = w_i$ $(i = 1, 2, \ldots, n)$, a_i is the cloud barycenter position vector, b_i is the cloud barycenter height vector, and w_i is the weight of the evaluation indicators. "$\times$"

represents the performance of the inner product operations. The deviation degree of the cloud barycenter was expressed as follows:

$$G' = (g_1', g_2', \ldots, g_n'). \tag{5}$$

(3) Determination of the weight of the indicators

Different index parameters had different effects, so it was necessary to select appropriate methods to determine the weight values of each indicator and to obtain the weight vector $w = [w_1, w_2, \ldots, w_n]$.

(4) Calculation of the deviation

Based on the ideal cloud barycenter vector, the deviation degree of each indicator g_i' was calculated:

$$g_i' = \begin{cases} \frac{(G_i - G_{i_0})}{G_{i_0}}, G_i < G_{i_0}\ i = 1, 2, \cdots, n \\ \frac{(G_i - G_{i_0})}{G_i}, G_i \geq G_{i_0} i = 1, 2, \cdots, n \end{cases}. \tag{6}$$

Then, the deviation of the combination weight σ was calculated using Equation (7):

$$\sigma = \sum_{i=1}^{n} g_i' w_i \ 0 < \sigma < 1. \tag{7}$$

(5) Determination of the health value

The health status of the system was expressed in different scores according to the deviations. The smaller the calculated weighted deviation, the closer the actual state of the evaluation object to the ideal state. The cloud model was used to represent the evaluation cloud generator obtained by each comment, as shown in Figure 3.

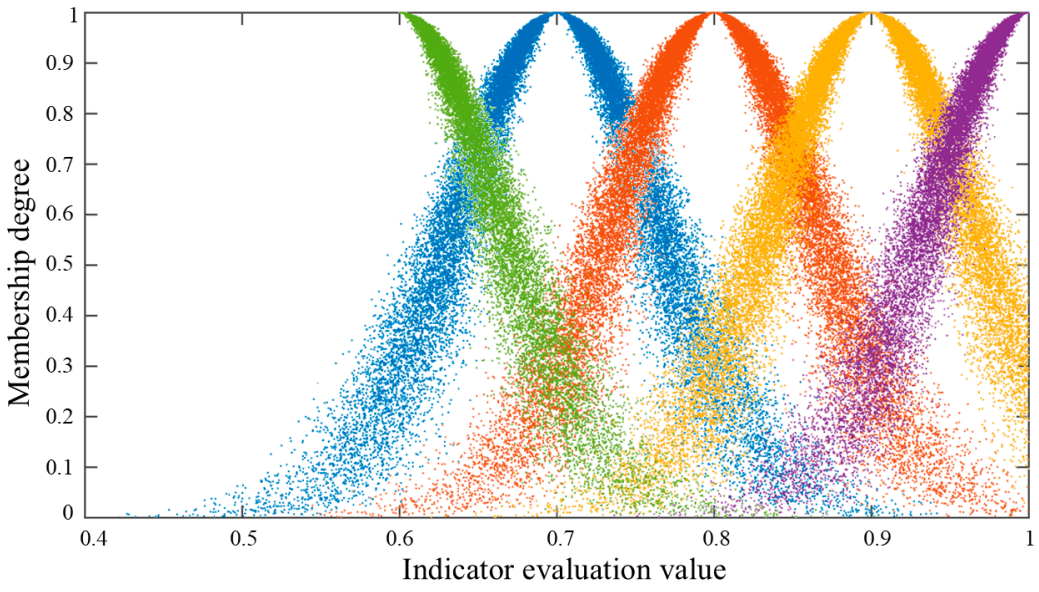


Figure 3. Assessment cloud model.

(1) Obtaining the assessment results

After the deviation degree σ was input into the cloud generator, if the activation degree of a comment cloud model was far greater than that of the other cloud models, then the health value could be considered to be the comment. If multiple cloud models were activated and the activation degree was almost the same, then a new assessment cloud model needed to be generated to obtain the expected value of the quantitative output result.

3.1.3. Improved Cloud Barycenter

The cloud barycenter method achieved the purpose of the health assessment by measuring the deviation degree between the current ideal states represented by σ. The traditional cloud barycenter method could only be applied to fixed indicators without restrictions; the other five indicators with certain restrictions were not applicable. Therefore, it was necessary to improve the calculation formula of $G_i{}'$, $(i = 1, 2, \ldots, m)$ according to the type of evaluation indicator [40,41].

According to the types of health indicators, the improved formulas were as follows:

For fixed indicators, $g_i{}'$ was calculated with Equation (6).

For cost indicators,

$$g_i{}' = \frac{G_i - G_{i_min}}{G_{i_max} - G_{i_min}}. \tag{8}$$

For interval indicators,

$$g_i{}' = \begin{cases} \frac{(G_i - G_{i_0_\max})}{(G_{i_\max} - G_{i_0_\max})}, G_i \geq G_{i_0_\max} \\ 0, G_{i_0_\min} < G_i < G_{i_0_\max} \\ \frac{(G_{i_0_\min} - G_i)}{(G_{i_0_\min} - G_{i_\min})}, G_i \leq G_{i_0_\min} \end{cases}, \tag{9}$$

where $G_{i_0_max}$ and $G_{i_0_min}$ are the upper and lower limits of the base data.

For benefit indicators,

$$g_i{}' = \frac{G_{i_\max} - G_i}{G_{i_\max} - G_{i_\min}}. \tag{10}$$

For deviation indicators,

$$g_i{}' = \begin{cases} \frac{(G_{i_max} - G_i)}{(G_{i_max} - G_{i_c})}, G_i \geq G_{i_c} \\ \frac{(G_i - G_{i_min})}{(G_{i_c} - G_{i_min})}, G_i < G_{i_c} \end{cases}, \tag{11}$$

where G_{i_c} is the fixed value in the indicators.

For deviations from interval-type indicators,

$$g_i{}' = \begin{cases} \frac{(G_{i_max} - G_i)}{(G_{i_max} - G_{i_c_\max})}, G_i \geq G_{i_c_\max} \\ \frac{(G_i - G_{i_min})}{(G_{i_c_\min} - G_{i_min})}, G_i < G_{i_c_\min} \end{cases}, \tag{12}$$

where $G_{i_c_max}$ and $G_{i_c_min}$ are the upper and lower limits of the interval.

Then, combined with the comprehensive weights ω_i of each indicator, the weighted deviation degree of the integrated cloud barycenter σ $(0 < \sigma < 1)$ was calculated according to Equation (13):

$$\sigma = \sum_{i=1}^{m} g_i{}' \omega_i. \tag{13}$$

For different types of indicators, the cloud barycenter deviation vectors were calculated with different methods, and the monitoring data for each indicator were compared with the reference values. If the deviation value calculated for each kind of indicator was between $[0, 1]$, it indicated that the equipment was running normally. If $\sigma > 1$ or $\sigma < 0$, it indicated that the monitoring value corresponding to the index had exceeded the upper or lower limit value, and some kind of fault had happened to the system.

3.2. Indicator System and Comprehensive Weight

In order to achieve a system condition assessment, different assessment purposes correspond to different indicators. For autonomous ships and smart engine rooms, there is

greater focus on whether the systems and equipment can fulfill the voyage requirements (port maintenance mode), specifically, whether the technical condition meets the basic functional needs for navigation. In the health assessment model, the selection of indicators directly affects the accuracy and reliability of the assessment. The main function of this part is to determine the evaluation indicators and the parameters of the system through the FAST method.

3.2.1. Indicator System

To be able to establish a reasonable indicator system, it was particularly important to understand the various functions of the system. Complex systems need different functions according to different purposes. The importance of each function is different, so it needs to be classified for different application scenarios. At the moment, the widely recognized division is into main, auxiliary, safeguarding, safety, hygienic, informative, connecting, and unnecessary functions [42]. The establishment of indicator system could be realized in four steps.

Step 1: Defining functions. The function of the system and its components were described in appropriate language.

Step 2: Functional analysis. The hierarchy and interaction of components were analyzed to determine the subordinate and parallel logical relationship between functions. According to the relationship between functions, it could be divided into three categories: main function, auxiliary function, and additional function.

Step 3: Functional Arrangement. On the basis of the logical relationship between the functions, they were arranged in the order of main function, auxiliary function, and additional function.

Step 4: Determining the indicator parameters. Firstly, the parameter which could best reflect or describe the technical performance of the system was taken as the indicator parameter, and then the optimal value (Baseline) [43] and threshold of the indicator were determined.

Using the FAST, the function of the systems and equipment was analyzed, the key components and corresponding functions were determined, and the function model diagram was established. Combined with the function model diagram, the specific process was analyzed, and the monitoring parameters that could represent the main function were determined in order to determine the indicator system [23].

3.2.2. Comprehensive Weight

To reduce the discrepancy between subjective and objective weights, a comprehensive weight was developed utilizing optimization theory.

It was assumed that there was a system with m assessment indicators and n monitoring objects, and the original data formed a two-dimensional relational matrix $R = (r_{ij})_{m\times n}$. After the dimensionless processing of R, the matrix $S = (s_{ij})_{m\times n}$ was obtained. The subjective and objective weights of the j indicator in the known system were ψ_j and φ_j, respectively. Here, ψ_j is the subjective weight, as calculated with fuzzy set theory [21,44], and φ_j is the objective weight, as calculated with the entropy weight method. The comprehensive weights of the combined optimization were ω_j. Then, the evaluation value of the first evaluation object was as follows:

$$f_i = \sum_{j=1}^{n} \omega_j s_{ij},\ j = 1, 2, \cdots, n. \tag{14}$$

For every item being evaluated in the system, a lower total deviation $F(\omega)$ signifies better evaluation results. Through the linear programming model Equation (15), the optimal comprehensive weight of the indicator could be obtained as follows:

$$\begin{cases} \min F(\omega) = \sum_{i=1}^{m} \sum_{j=1}^{n} \left(\left[(\psi_j - \omega_j) s_{ij} \right]^2 + \left[(\varphi_j - \omega_j) s_{ij} \right]^2 \right) \\ s.t. \ \ \sum_{j=1}^{n} \omega_j = 1, \ \omega_j \geq 1 \end{cases} . \tag{15}$$

3.3. Dynamic Reliability Assessment of a System

The sliding time window was introduced to update the data dynamically, and real-time online calculation of the health indicator has been successfully executed.

The size of the sliding data window was established using the Kolmogorov–Smirnov (K-S) test to ascertain whether the measurement parameter within the window adheres to a normal distribution. To realize the dynamic health assessment by the sliding time window, it was necessary to determine the number of data groups in the sliding window, that is, the window size. In this research, the average of the data in the sliding time window was taken as the cloud barycenter vector, shown in Figure 4, which represented the state parameters of the current evaluation object. The larger the window size, the higher the delay of the evaluation results, and the less timely the reflection of the changes in the health status. At the same time, too large of a window size would reduce the impact of a single group of data on the calculation results; that is, it would reduce the sensitivity of the model.

Correlation coefficient analysis depicted in Figure 5 was used to determine the length of the window when the dynamic health value was calculated. When the window length is greater than 10 min, the correlation coefficient has almost no change. If the length of the selection window is more than 10 min, the number of training samples will increase and the amount of calculation will also increase. Therefore, the window length was selected as 10 min. The data acquisition cycle of the marine systems was 10 s, and the data length in the window was 60.

Considering the measurement and the uncertainty of the system, the dynamic update of the weight and real time calculation of the health value were achieved by using the sliding time window and the cloud barycenter model.

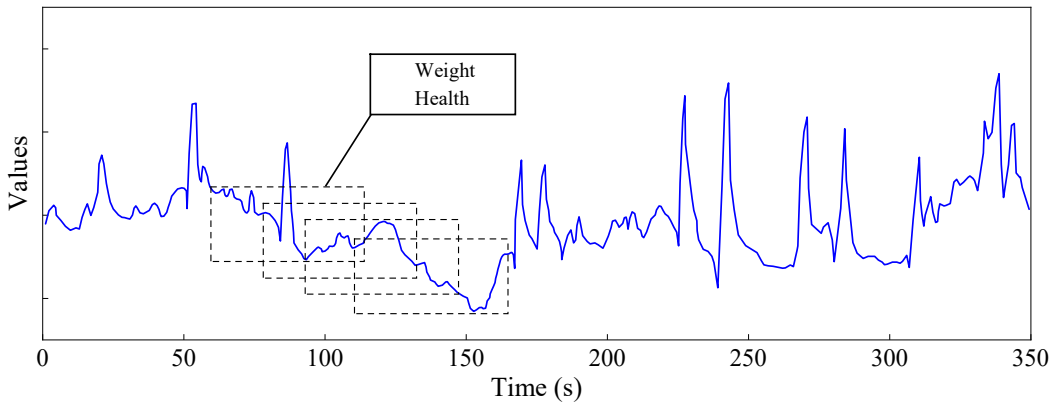


Figure 4. Dynamic weight and health value calculation.

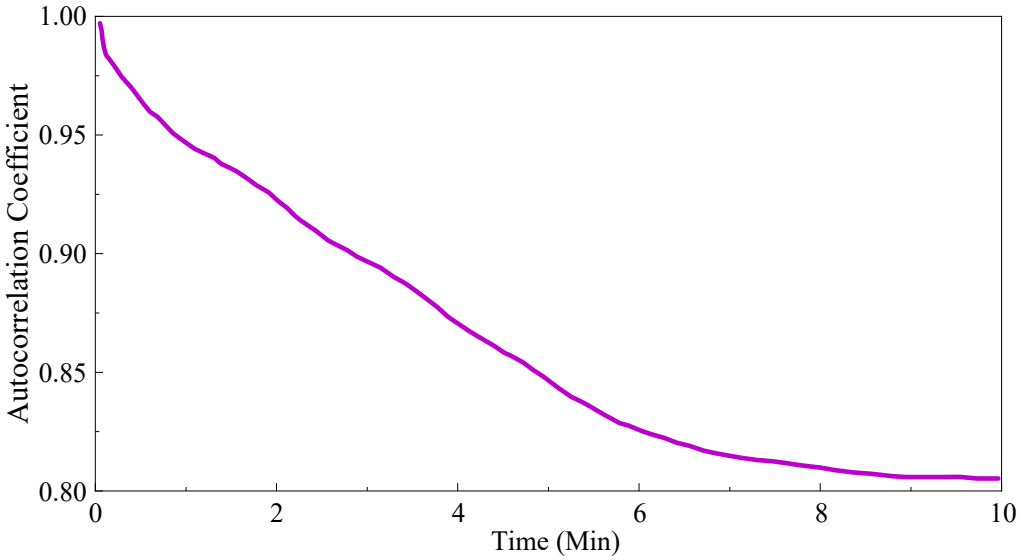


Figure 5. Autocorrelation analysis.

3.4. Reliability Analysis of Health Value

The health value obtained by the dynamic health model in this research reflected the comprehensive state of the whole system, and it could not reflect the health state information of a specific piece of equipment. Therefore, it was necessary to evaluate the reliability of the assessment results to avoid the extreme situation caused by the deviation between each piece of equipment. According to the principle of the cloud barycenter, the deviation g_i' between the actual monitoring value of each index parameter and the benchmark could reflect the health status of the corresponding equipment. Based on the comprehensive deviation degree σ, combined with the deviation degree g_i' for each piece of equipment, the dispersion degree of the health value was calculated. The health status of each piece of sub equipment might be considered in a balanced way to prevent the occurrence of extreme cases where the deviation value of one piece of equipment was far greater than that of the other pieces of equipment (the system could be used due to the failure of an individual piece of equipment). The dispersion of the system health value was calculated as follows:

$$S = \sqrt{\frac{\sum_{i=1}^{n} (g_i' - \sigma)^2}{n-1}}. \quad (16)$$

4. Case Study

4.1. System Description

Marine piping systems are used to connect various types of mechanical equipment and to transport water, oil, gas, and other related working substances on ships. Most of the equipment in a system can achieve automatic control according to the requirement of an intelligent ship. In this case study, the FOSS was selected as the research object, and the feasibility of the method was verified. All of the data described in the following sections were from real ship operation parameters (from a training ship).

4.2. Implementation of the Method

The FOSS is tasked with supplying appropriate fuel for combustion. Any problem within the system will directly influence the operation of the ship's propulsion system, subsequently influencing the reliability of the entire ship. The system is composed of many components, i.e., a duplex filter (DF), supplying pump (SP), circulating pump (CP), auto-filter (AF), atomizing heater (HT), oil mixing box (MB), pipeline, and accessories. Figure 6

depicts the structure of the system. The FOSS has two working modes, diesel oil mode and fuel oil mode. Two distinct pattern recognition methodologies utilize the positional configurations of three-way valves as primary discriminative features for operational mode classification because the fuel oil is the key mode of the ship, and the health value is based on this mode.

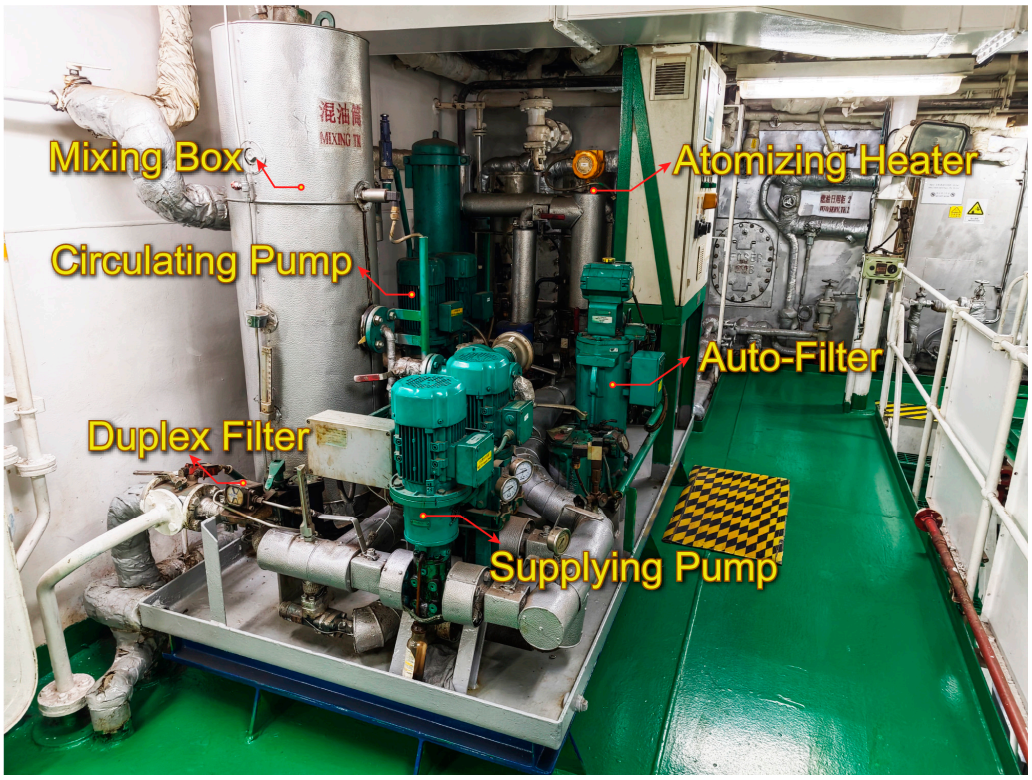


Figure 6. The composition of the FOSS.

4.2.1. Condition Assessment Indicator System

This section describes how the FAST method was adopted to analyze the relevant influencing factors through the analysis of the specific functions of the system and equipment, and the influencing factors were classified to establish an assessment indicator system. The specific implementation steps were as follows:

(1) System functions

The main engine FOSS dealt with the fuel so that the fuel oil flow, impurities, viscosity, and pressure could meet the requirements to ensure the combustion effect of the main engine. The functions of the whole system were as follows:

Step 1: Purification. The primary DF and the secondary AF were used to purify the fuel.

Step 2: Heating. The HT was used to heat the fuel to the proper viscosity.

Step 3: Pressurization. The SP and the CP are used to pressurize fuel.

Step 4: Mixing. The MB was used to mix the fuel oil and the diesel oil.

Step 5: Circulating. The pumps and pipeline were used to cycle the fuel to make the engine start at any time.

(2) Functional analysis

Through the classification of the relationship between the various equipment and the components in the system, the relationship diagram could be established as shown in Figure 7, and the importance and the relationship between the functions could be analyzed.

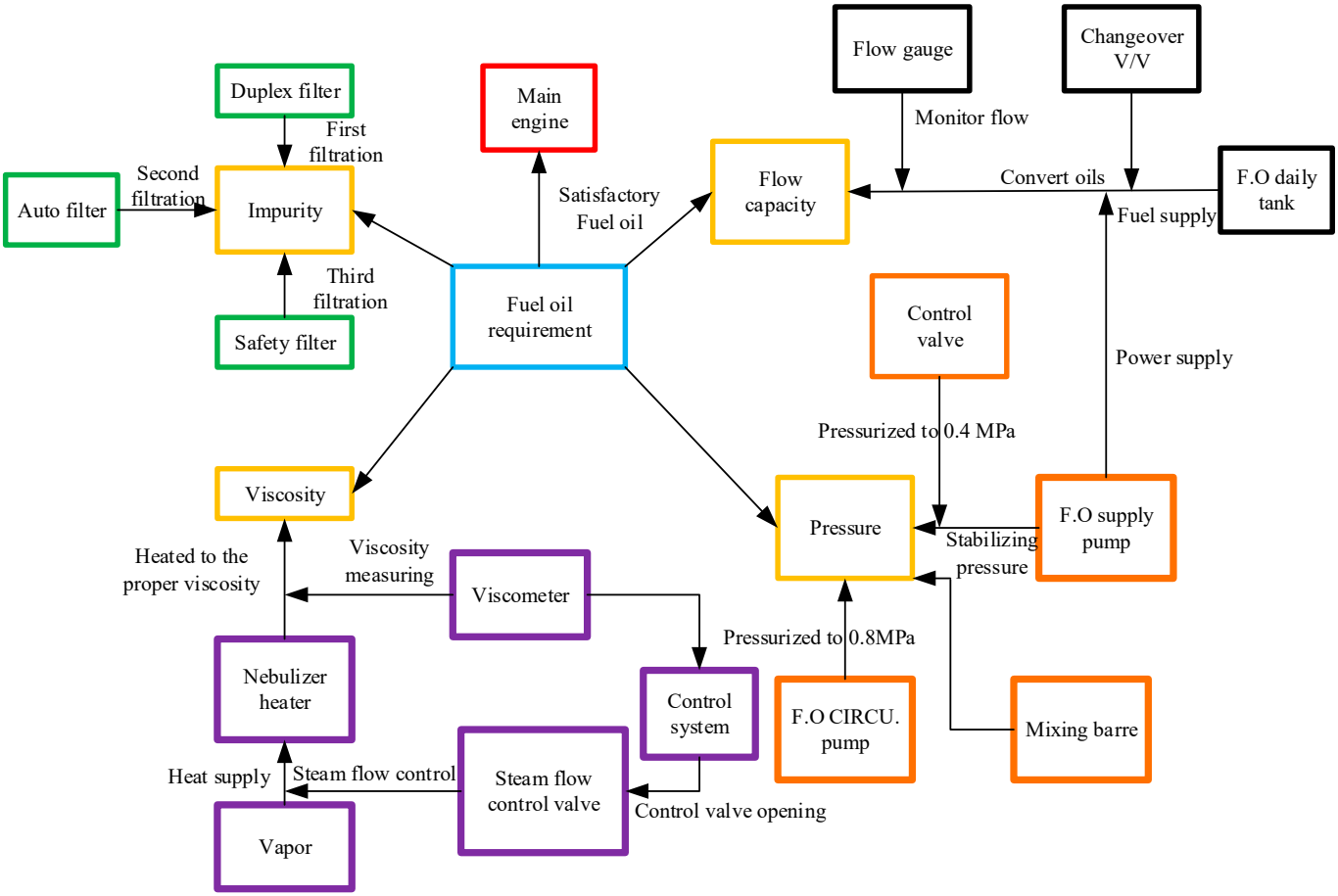


Figure 7. The function of the FOSS.

(3) Functional arrangement

According to the analysis of the importance and the relationship in Figure 8, the system had four main functions: oil conversion, fuel heating, fuel purification, and fuel pressurization. The parameters related to the four main functions of the system were the most representative in reflecting the health status of the whole system. The main functions were as follows:

Step 1: The function of oil conversion was accomplished by the change in the three-way valve position.

Step 2: The heating of the fuel was accomplished through heat exchange between the fuel and the saturated steam. The amount of heat exchanged in the heat transfer process depended on the amount of saturated steam that could enter the heaters. The control box of the main engine FOSS controlled the amount of saturated steam by controlling the opening degree of the valve at the intake pipe.

Step 3: Fuel purification involved forcing the fuel to pass through the DF and AF under the action of the pressure difference in order to achieve the purpose of physical filtration. Since the accuracy of the filter was fixed, under normal circumstances, the pressure difference before and after the filter had to be within a certain range. Moreover, the blockage or breakage of the filter screen would lead to the change in the pressure difference between the inlet and the outlet.

Step 4: The function of fuel pressurization was to pressurize the fuel. At the same time, this function could also maintain the stable inlet pressure.

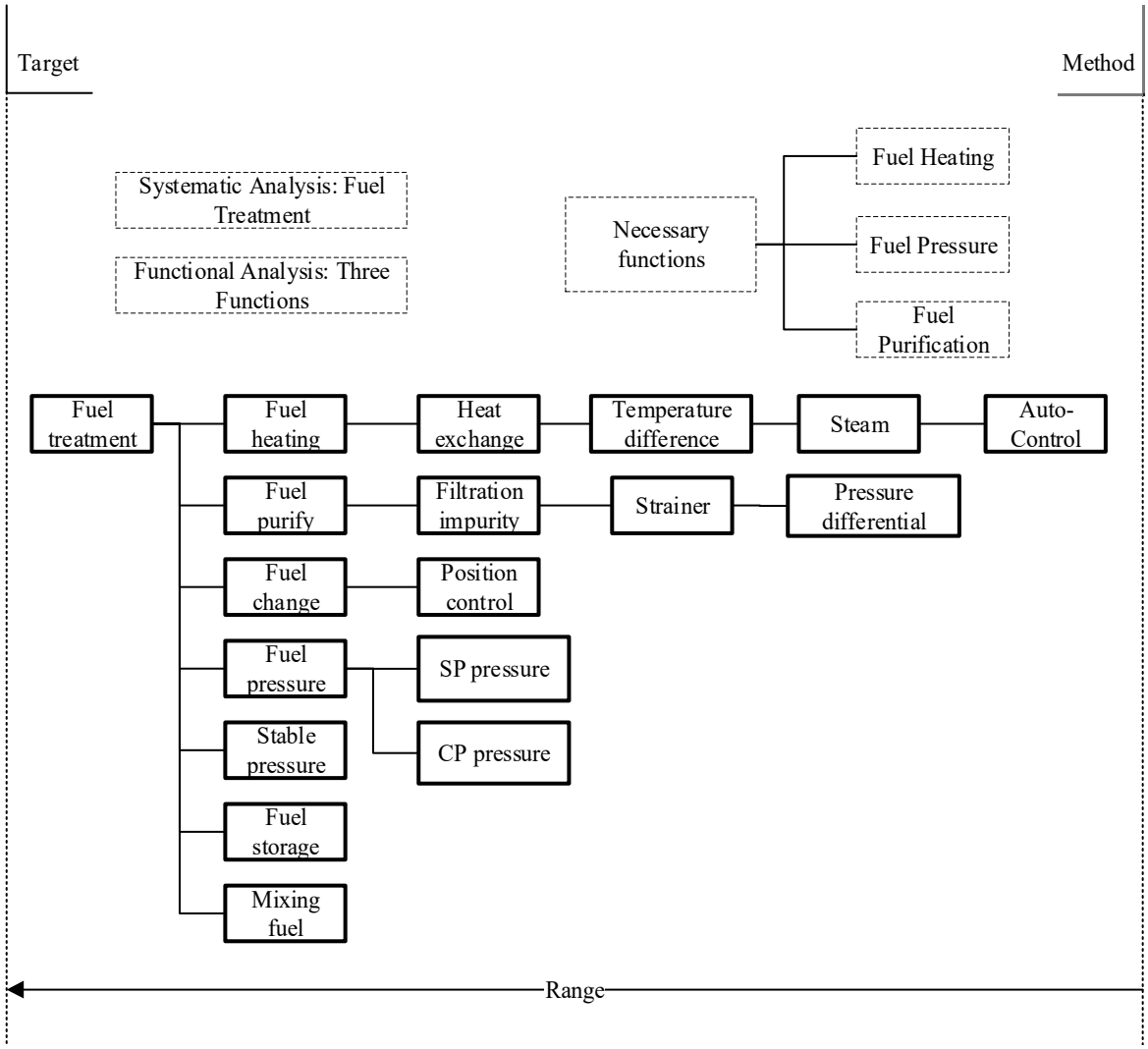


Figure 8. Functional arrangement of the FOSS.

(4) Determining indicator parameters

FOSS had two working modes, diesel oil mode and fuel oil mode. Two kinds of pattern recognition were based on the valve position of the three-way valve because the fuel oil was the key mode of the ship, and the health value was based on this mode.

Step 1: The fuel oil was successfully heated using an atomizing heating mechanism, which is a combination of a heater and an automatic control protocol. The essential role of this device is to maintain the fuel viscosity within the desired range, making fuel viscosity an essential parameter.

Step 2: The purification of fuel oil was realized by the filtering effect of the filters. With the increase in service time, the filters were dirty, and the pressure of fuel through the filters decreased. Therefore, the changes in the pressure difference in the DF and AF were selected as the key parameters.

Step 3: In the context of fuel pressurization, SP was employed to keep the fuel pressure constant, and CP was used to raise the fuel pressure. As a result, the fuel pressures at the exits of SP and CP emerged as key indicators. Through the analysis of the functions and parameters of the key equipment of the system, the evaluation indicator system is shown in Figure 9.

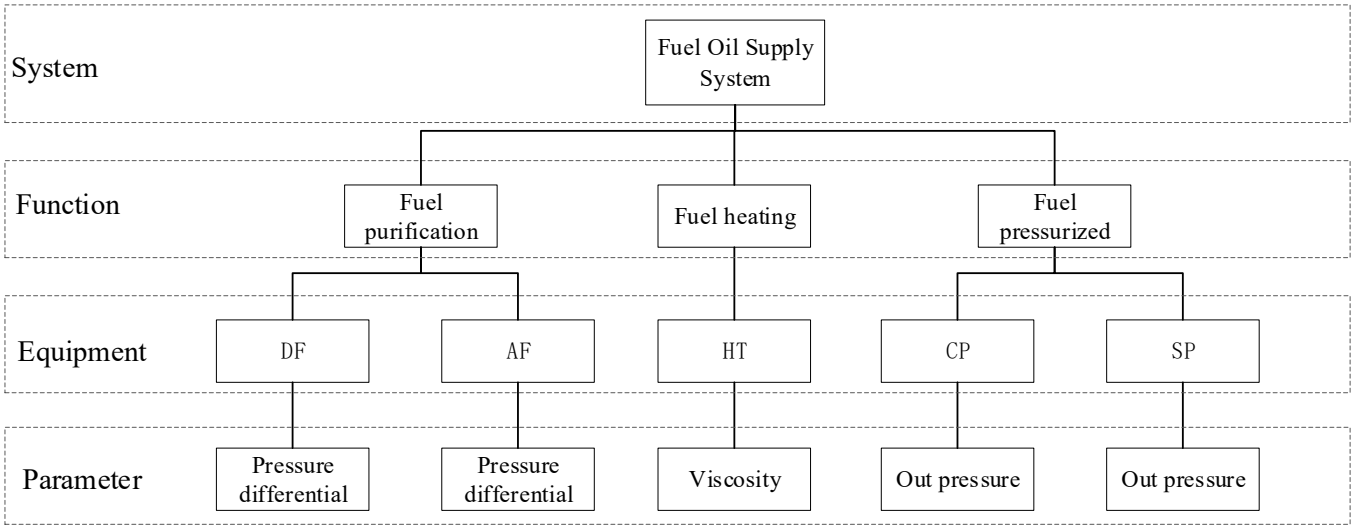


Figure 9. Health assessment indicator system for the FOSS.

(5) Determining the datum of the parameters

The set-up of the threshold for the filters was often a decision based on factory test results in the specifications. The threshold of the pump outlet pressure came from the actual test results of the ship system (sea trial), and the heater threshold depended on the fuel temperature–viscosity characteristic curve and fuel types. The details of the equipment threshold that was considered are shown in Table 1.

Table 1. Benchmarks of health assessment indicators for FOSS.

Equipment	Parameter	Type	Unit	Threshold		
				Lower Limit	Optimal	Upper Limit
DF	Δp_1	Cost	bar	0.2	0.2	0.8
AF	Δp_2	Cost	bar	0.2	0.3	0.8
HT	V	Interval	cSt	7.0	12.0–14.0	20.0
SP	p_1	Fixed	bar	3.0	5.0	5.0
CP	p_2	Fixed	bar	6.0	8.0	11.0

4.2.2. Weight Calculation

(1) Subjective weight

According to the basic principle of the FS method, the subjective weight was calculated. The weight set values of the indicators are shown in Table 2.

Table 2. Weight set values of the indicators.

Expert	Indicator System				
	DF Δp_1	AF Δp_2	HT V	SP p_1	CP p_2
E_1	10–20	10–20	15–25	20–30	20–30
E_2	5–15	10–20	25–35	10–20	25–35
E_3	5–15	10–20	20–30	30–40	10–20
E_4	1–10	10–20	15–25	20–35	20–35
E_5	5–18	14–25	25–35	15–28	18–26
E_6	20–30	20–28	15–25	13–20	13–20
E_7	1–10	1–10	20–40	20–40	20–40
E_8	12–17	8–12	22–28	18–22	28–32

In order to make the weights of the indicators comprehensive, three levels of consulting were selected, including the shipping company, management personnel, and the marine engineers. According to the different positions, experience, and knowledge structure, expert opinions were classified as shown in Table 3.

$$k_i = \frac{s_i}{\sum_{i=1}^{q} s_i}, \tag{17}$$

where k_i is the weight value, s_i is the score value of the expert i, and q is the number of experts.

Table 3. Grading and scoring for expert opinions.

Opinion Level	Class A	Class B	Class C
Score	3	2	1
Duty	Chief engineer	Second engineer	Third (Fourth) engineer

The weights of the expert opinions were obtained as shown in k = [0.07, 0.13, 0.20, 0.13, 0.20, 0.07, 0.13, 0.07]. Therefore, the subjective weights of the indicators were ψ = [0.10, 0.15, 0.26, 0.25, 0.24].

(2) Objective weight

According to the principle of the entropy weight method, the objective weights were calculated based on the sliding time window size. The calculation results are shown in Figure 10.

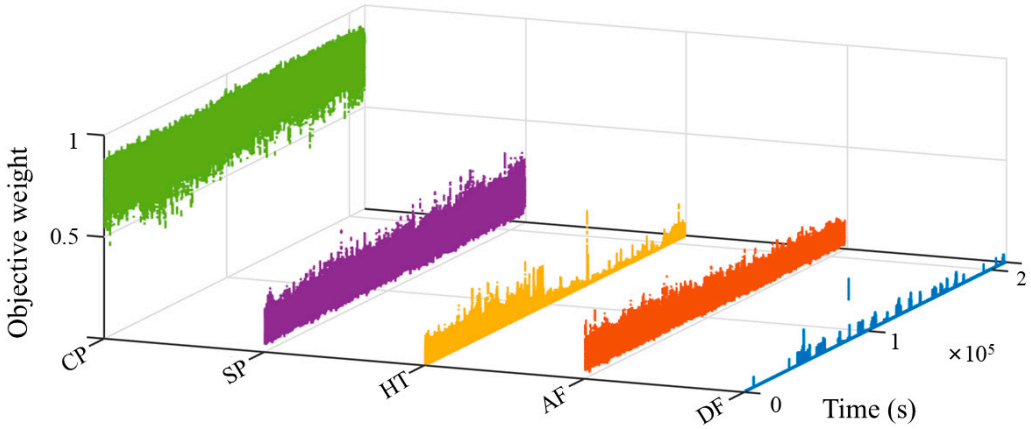


Figure 10. Objective weight variation with parameters.

(3) Combination weight

According to the principle of deviation minimization described in Section 3.2.2, the optimal comprehensive weight value was obtained. The objective weight varied with the changes in the equipment state parameters in the sliding window, and the comprehensive weight changed.

4.2.3. Continuous Online Condition Assessment

The monitoring data from January to July corresponding to the system indicator parameters were extracted from the real ship database. Before calculating the health value, data preprocessing was necessary. Outliers and downtime in the dataset were filtered. According to the dynamic cloud barycenter method, the cloud barycenter deviation of each piece of equipment was calculated, as shown in Figure 11.

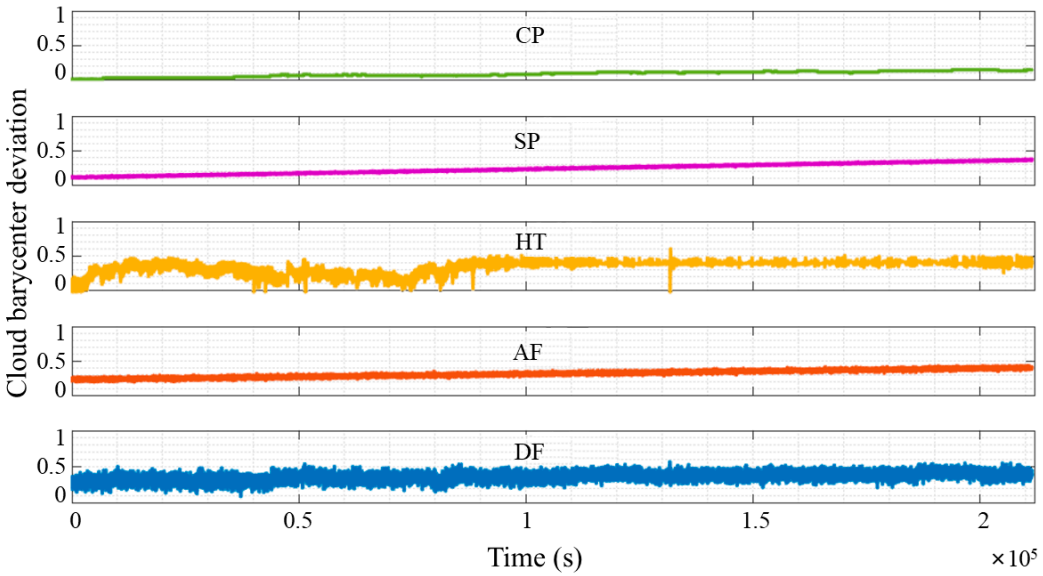


Figure 11. Cloud barycenter deviation of equipment.

Figure 12 illustrates the decision-making of CBM according to different degradation stages. If the system functional degradation is between the A. Point and the E. Point through health monitoring, the possible decision can be made to avoid the failure. The formulation of limits often hinges on practical engineering knowledge, the study of historical data, and established standards within the industry. The adaptive threshold could be calculated dynamically according to the data prediction model. Condition-based maintenance can effectively prevent system failure and reduce operation and maintenance costs.

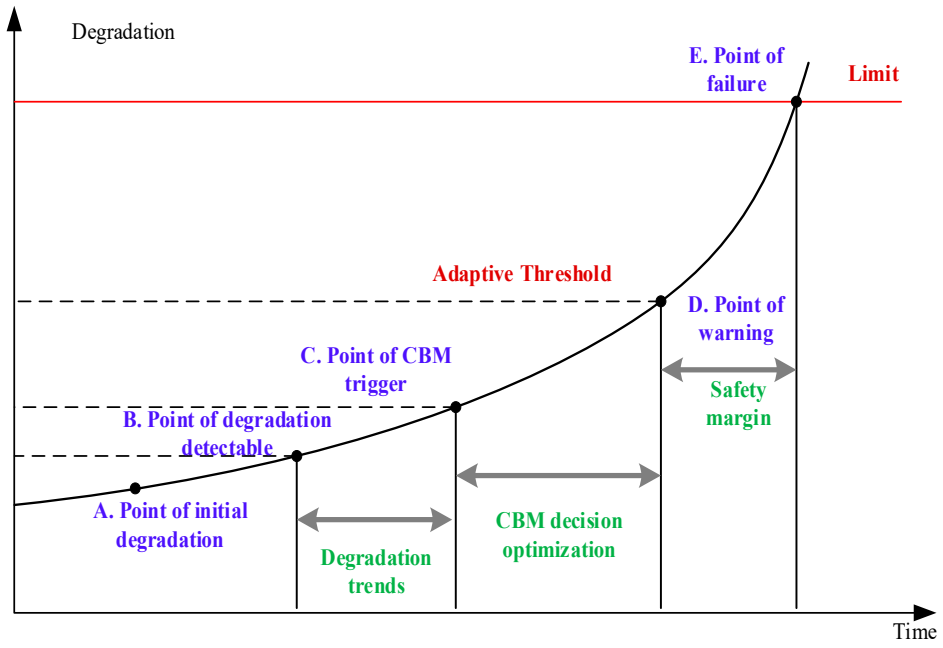


Figure 12. CBM decision.

H = 100 indicated the optimal operation and H = 60 meant a fault condition. H = 90, 80, and 70, respectively, correspond to the deviation degree of health value from the optimal state. The data in this research were for the state parameters obtained after the system had been running for a period. According to Figure 13, before the B. point, the equipment and components were in the running-in period, the health value decreased rapidly, and the duration was short. The health value at the onset was situated between 90 and 100. With

the extension of time, the system showed an obvious degradation process and the health value corresponded to 80–90. After the C. point, the health value was lower than 80 points. It could be seen that between the C. point and the D. point, engineers and experts could make corresponding operation and maintenance decisions according to the change speed and trend of health value. For the stage between the D. point and the E. point, although the system could still complete all or part of the function, it might fail at any time, leading to the loss of function. When the health value was at point D, the system was in the failure stage. Certain equipment and components were not functioning normally, leading to an impact on the system's overall health value.

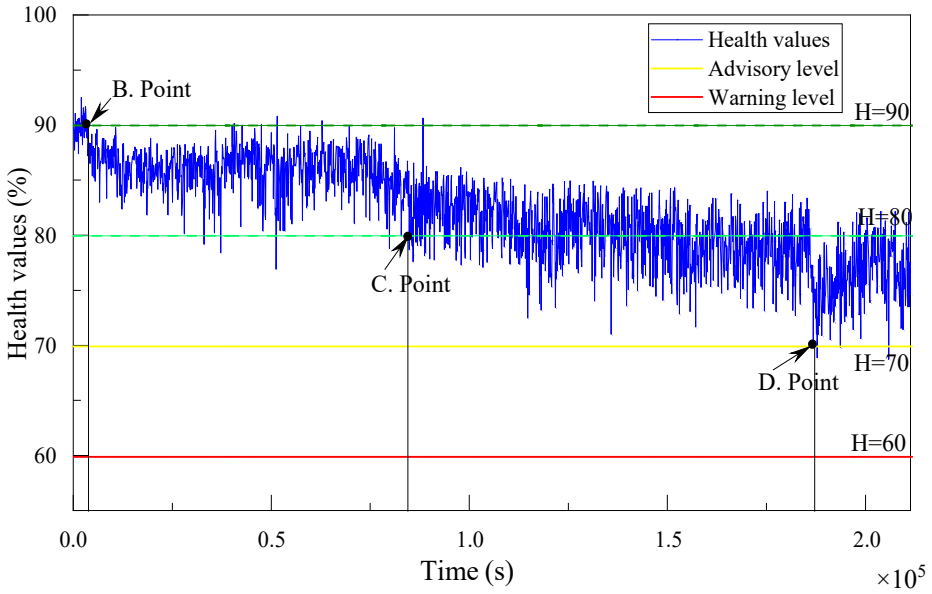


Figure 13. Health values for FOSS.

According to Equation (16), the health value departure curve of FOSS under long-time operation is calculated and obtained, as shown in Figure 14. The dispersion of the health value remains below 0.20, which indicates that there is no significant abnormality of individual equipment. Consequently, the evaluation finding is dependable, and the health value serves as an indicator of the system's overall health situation.

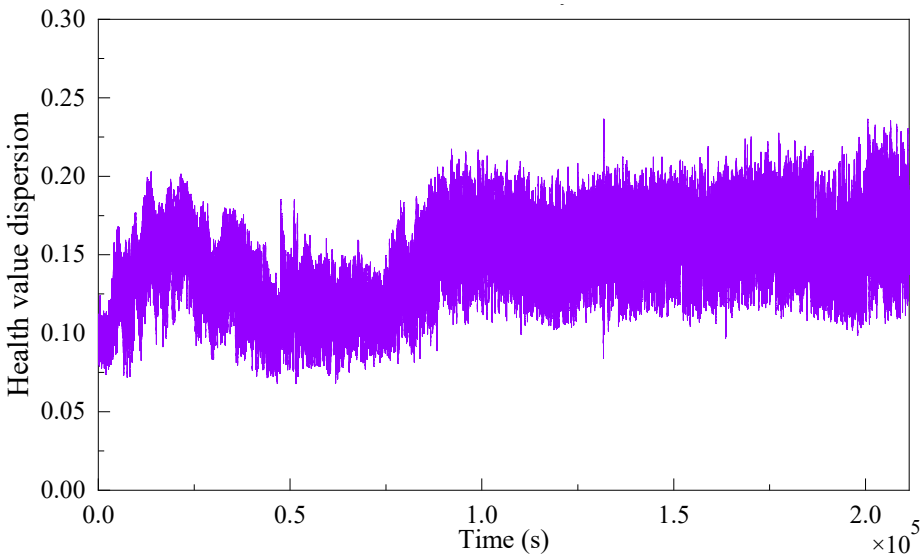


Figure 14. Health value dispersion of FOSS.

4.3. Comments and Discussions

Traditional mechanical system health assessments predominantly relied on static assessment methods, which utilized historical data to approximate the system's current state but could not facilitate real-time health state monitoring. In contrast, dynamic evaluation can be adapted in real-time based on parameter changes, yielding assessment results that more closely mirror actual changes and providing valuable input for CBM and decision-making support.

The suggested approach offered a comprehensive health assessment by combining the probability health indicators of individual components. The system's condition was assessed using multiple related signals, enabling the detection of potential faults. Especially in the context of intelligent engine rooms or unmanned ships, emphasis was placed on the duration during which systems and equipment could fulfill their functional output and operate continuously. In cases where individual equipment within the system encountered issues or performance decline, the essential functions of the entire system remained effective, which was crucial for making operational and maintenance decisions.

As shown in Figure 15, the system featuring fixed weights would first hit the specified limit (health value = 60), activating the maintenance routine. Upon inspection of the dismantled FOSS, it was revealed that the DF of the system was fouled, causing a decrease in the system's health value. Despite this, the system's output pressure and flow remained unaffected, continuing to fulfill the demands of the marine diesel engine. The health value assessed by the dynamic health model aligns more precisely with the system's operational reality.

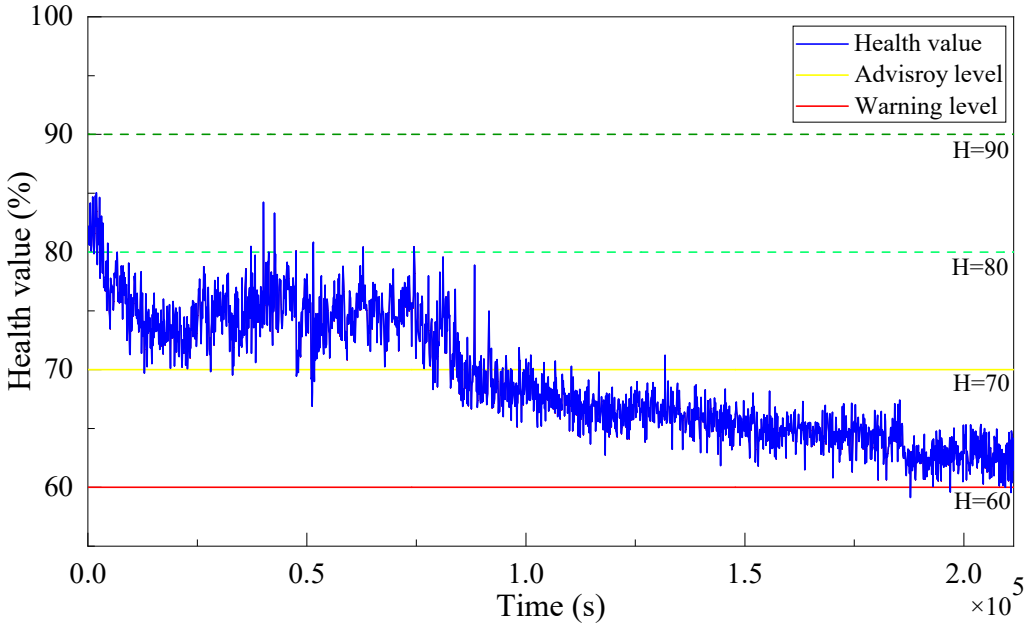


Figure 15. Fixed weight health values comparison.

The dynamic health model is applicable to the calculation of system health values in single mode. Multi-mode operational systems require implementing either novel pattern recognition architectures or leveraging existing identification frameworks for robust data categorization, subsequently enabling health index quantification through dynamic model-based analytics. Furthermore, before the analytics, the index data need to be processed to eliminate the influence of singular value on health value.

5. Conclusions

Intelligent ships are ushering in a new operation and maintenance paradigm, necessitating a more precise understanding of system health status changes. Consequently, quantifying system health status and tracking its evolution have become critical research areas for intelligent operation and maintenance decision-making. This paper addresses the growing demand for health status monitoring in intelligent and unmanned ship systems. By analyzing the functions and characteristics of ship systems, the study proposes a dynamic health status evaluation method based on cloud centroid assessment. This method comprehensively considers the impact of inherent factors, such as system structure and equipment quality, as well as subjective and objective uncertainties. It also accounts for the intrinsic relationship between randomness and fuzziness in complex systems, achieving a coupling of subjective and objective factors. By mapping the health evolution process to discrete health values, the method quantifies the system's health status and, through dynamic modeling, enables continuous online evaluation. Compared to static evaluation approaches, the proposed dynamic health status assessment method better adapts to health status changes and supports continuous online monitoring. Validation based on system performance output and disassembly inspection results demonstrates that the dynamic evaluation results more accurately reflect the true health status of the system. These results can serve as a reliable benchmark for operation and maintenance decision-making, offering significant practical value for intelligent ship management.

Although the study has achieved dynamic assessment of system health status, several issues remain to be addressed for further improvement. First, the evaluation process in the paper relies on a fixed threshold. If an adaptive threshold could be established based on the system's health evolution, the accuracy of the assessment results could be significantly enhanced. This represents a key area for future research. Second, the verification of evaluation results currently combines actual ship system performance output and disassembly inspections. While effective, this approach lacks universality. Developing a standardized evaluation system with unified indicators would better validate the method's effectiveness and applicability, which also warrants further investigation.

Author Contributions: L.G. and T.W. contribute equally to this work. Conceptualization, L.G. and P.Z.; methodology, L.G., T.W., and X.D.; software, P.Z. and H.Z.; validation, T.W. and L.G.; data curation, T.W. and X.D.; writing—original draft preparation, L.G.; writing—review and editing, P.Z., H.Z., and J.Z.; supervision, J.Z. and H.Z. All authors have read and agreed to the published version of the manuscript.

Funding: This research was funded by the High Technology Ship Research and Development Program, project "Development of liquid cargo and electromechanical simulation operation system for LNG Ship" (Grant No. CBG3N21-3-3), and the Intelligent Ship Engine Room Simulation Teaching Experimental Platform Project (Grant No. 9223136).

Institutional Review Board Statement: Not applicable.

Informed Consent Statement: Not applicable.

Data Availability Statement: Data are available by reasonable request from corresponding authors.

Conflicts of Interest: The authors declare no conflicts of interest.

References

1. Thieme, C.A.; Utne, I.B. Safety performance monitoring of autonomous marine systems. *Reliab. Eng. Syst. Saf.* **2017**, *159*, 264–275. [CrossRef]
2. Jardine, A.K.S.; Lin, D.; Banjevic, D. A review on machinery diagnostics and prognostics implementing condition-based maintenance. *Mech. Syst. Signal Process.* **2006**, *20*, 1483–1510. [CrossRef]

3. Wang, W.; Kobbacy, K.; Murthy, D. *Condition-Based Maintenance Modelling, Complex System Maintenance Handbook*; Springer: London, UK, 2008.
4. Jing, L.; Zhao, M.; Li, P.; Xu, X. A convolutional neural network based feature learning and fault diagnosis method for the condition monitoring of gearbox. *Measurement* **2017**, *111*, 1–10. [CrossRef]
5. Lei, Y.; Li, N.; Guo, L.; Li, N.; Yan, T.; Lin, J. Machinery health prognostics: A systematic review from data acquisition to RUL prediction. *Mech. Syst. Signal Process.* **2018**, *104*, 799–834. [CrossRef]
6. Cocozza-Thivent, C.; Eymard, R.; Mercier, S. A finite-volume scheme for dynamic reliability models. *IMA J. Numer. Anal.* **2006**, *26*, 446–471. [CrossRef]
7. Lin, Y.-H.; Li, Y.-F.; Zio, E. Fuzzy Reliability Assessment of Systems With Multiple-Dependent Competing Degradation Processes. *IEEE Trans. Fuzzy Syst.* **2015**, *23*, 1428–1438. [CrossRef]
8. Wang, H.; Hong, R.; Chen, J.; Tang, M. Intelligent Health Evaluation Method of Slewing Bearing Adopting Multiple Types of Signals from Monitoring System. *Int. J. Eng. Trans. A Basics* **2015**, *28*, 573–582.
9. Wang, J.; Zhang, L.; Zheng, Y.; Wang, K. Adaptive prognosis of centrifugal pump under variable operating conditions. *Mech. Syst. Signal Process.* **2019**, *131*, 576–591. [CrossRef]
10. Wang, D.; Tse, P.W. Prognostics of slurry pumps based on a moving-average wear degradation index and a general sequential Monte Carlo method. *Mech. Syst. Signal Process.* **2015**, *56–57*, 213–229. [CrossRef]
11. Yang, H.-H.; Huang, M.-L.; Lai, C.-M.; Jin, J.-R. An approach combining data mining and control charts-based model for fault detection in wind turbines. *Renew. Energy* **2018**, *115*, 808–816. [CrossRef]
12. Liang, T.; Meng, Z.; Xie, G.; Fan, S. Multi-Running State Health Assessment of Wind Turbines Drive System Based on BiLSTM and GMM. *IEEE Access* **2020**, *8*, 143042–143054. [CrossRef]
13. Hu, A.; Bai, Z.; Lin, J.; Xiang, L. Intelligent condition assessment of industry machinery using multiple type of signal from monitoring system. *Measurement* **2020**, *149*, 107018. [CrossRef]
14. Nguyen, K.T.P.; Phuc, D.; Tuan, H.K.; Berenguer, C.; Grall, A. Joint optimization of monitoring quality and replacement decisions in condition-based maintenance. *Reliab. Eng. Syst. Saf.* **2019**, *189*, 177–195. [CrossRef]
15. Azadeh, A.; Sheikhalishahi, M.; Khalili, S.M.; Firoozi, M. An integrated fuzzy simulation-fuzzy data envelopment analysis approach for optimum maintenance planning. *Int. J. Comput. Integr. Manuf.* **2014**, *27*, 181–199. [CrossRef]
16. Barabady, J.; Kumar, U. Reliability analysis of mining equipment: A case study of a crushing plant at Jajarm Bauxite Mine in Iran. *Reliab. Eng. Syst. Saf.* **2008**, *93*, 647–653. [CrossRef]
17. Azadeh, A.; Seif, J.; Sheikhalishahi, M.; Yazdani, M. An integrated support vector regression-imperialist competitive algorithm for reliability estimation of a shearing machine. *Int. J. Comput. Integr. Manuf.* **2016**, *29*, 16–24. [CrossRef]
18. Azadeh, A.; Asadzadeh, S.M.; Seif, J. An integrated simulation-analysis of variance methodology for effective analysis of CBM alternatives. *Int. J. Comput. Integr. Manuf.* **2014**, *27*, 624–637. [CrossRef]
19. Rana, M.M.; Xiang, W.; Wang, E. Smart grid state estimation and stabilization. *Int. J. Electr. Power Energy Syst.* **2018**, *102*, 152–159. [CrossRef]
20. Sun, J.; Wang, F.; Ning, S. Aircraft air conditioning system health state estimation and prediction for predictive maintenance. *Chin. J. Aeronaut.* **2020**, *33*, 947–955. [CrossRef]
21. Li, H.; Hu, Y.G.; Yang, C.; Chen, Z.; Ji, H.T.; Zhao, B. An improved fuzzy synthetic condition assessment of a wind turbine generator system. *Int. J. Electr. Power Energy Syst.* **2013**, *45*, 468–476. [CrossRef]
22. Zhao, Y.; Li, D.; Dong, A.; Kang, D.; Lv, Q.; Shang, L. Fault Prediction and Diagnosis of Wind Turbine Generators Using SCADA Data. *Energies* **2017**, *10*, 1210. [CrossRef]
23. Liu, Y.; Zuo, M.J.; Li, Y.-F.; Huang, H.-Z. Dynamic Reliability Assessment for Multi-State Systems Utilizing System-Level Inspection Data. *IEEE Trans. Reliab.* **2015**, *64*, 1287–1299. [CrossRef]
24. Moghaddass, R.; Zuo, M.J.; Liu, Y.; Huang, H.-Z. Predictive analytics using a nonhomogeneous semi-Markov model and inspection data. *IIE Trans.* **2015**, *47*, 505–520. [CrossRef]
25. Lie, J.; Zio, E. System dynamic reliability assessment and failure prognostics. *Reliab. Eng. Syst. Saf.* **2017**, *160*, 21–36. [CrossRef]
26. Xing, J.; Zeng, Z.; Zio, E. A framework for dynamic risk assessment with condition monitoring data and inspection data. *Reliab. Eng. Syst. Saf.* **2019**, *191*, 106552. [CrossRef]
27. Zhang, Y.; Zhang, P.; Zhang, B.; Sun, P. Health Condition Assessment of Marine Systems Based on an Improved Radar Chart. *Math. Probl. Eng.* **2020**, *2020*, 8878908. [CrossRef]
28. You, L.; Zhang, J.; Li, Q.; Ye, N. Structural reliability analysis based on fuzzy random uncertainty. *Eksploat. I Niezawodn. -Maint. Reliab.* **2019**, *21*, 599–609. [CrossRef]
29. Koc, M.L.; Koc, D.I. A cloud theory based reliability analysis method and its application to reliability problems of breakwaters. *Ocean. Eng.* **2020**, *209*, 107534. [CrossRef]
30. Wang, Z.; Huang, H.-Z.; Li, Y.; Pang, Y.; Xiao, N.-C. An approach to system reliability analysis with fuzzy random variables. *Mech. Mach. Theory* **2012**, *52*, 35–46. [CrossRef]

31. He, Y.; Zhao, Y.; Han, X.; Zhou, D.; Wang, W. Functional risk-oriented health prognosis approach for intelligent manufacturing systems. *Reliab. Eng. Syst. Saf.* **2020**, *203*, 107090. [CrossRef]
32. Li, D.; Cheung, D.; Shi, X.M.; Ng, V. Uncertainty reasoning based on cloud models in controllers. *Comput. Math. Appl.* **1998**, *35*, 99–123. [CrossRef]
33. Li, D.; Liu, C.; Gan, W. A New Cognitive Model: Cloud Model. *Int. J. Intell. Syst.* **2009**, *24*, 357–375. [CrossRef]
34. Kavousi-Fard, A.; Niknam, T.; Fotuhi-Firuzabad, M. A Novel Stochastic Framework Based on Cloud Theory and theta-Modified Bat Algorithm to Solve the Distribution Feeder Reconfiguration. *IEEE Trans. Smart Grid* **2016**, *7*, 740–750.
35. Yang, H.; Xu, G.; Fan, X. A reliability analysis method of cloud theory—Monte Carlo based on performance degradation data. *Eksploat. I Niezawodn. Maint. Reliab.* **2015**, *17*, 435–442. [CrossRef]
36. Zhang, C.; Shi, Q.; Liu, T. Air base damage evaluation using cloud barycenter evaluation method. In *Frontiers of Advanced Materials and Engineering Technology*; Pts 1–3; Chen, R., Sun, D., Sung, W.P., Eds.; Trans Tech Publications: Bäch, Switzerland, 2012; pp. 803–807.
37. Zhang, C.; Shi, Q.; Liu, T. Study on Application of Cloud Barycenter Evaluation Method to Battle Damage Assessment. *Comput. Simul.* **2012**, *29*, 28–31.
38. Li, D.; Liu, C.; Du, Y.; Han, X. Artificial Intelligence with Uncertainty. *J. Softw.* **2004**, *15*, 1583–1594.
39. Wang, G.; Xu, C. Cloud Model-A Bidirectional Cognition Model between Concept's Extension and Intension. In *Advanced Machine Learning Technologies and Applications*; Hassanien, A.E., Salem, A.B.M., Ramadan, R., Kim, T.H., Eds.; Springer: Berlin/Heidelberg, Germany, 2012; pp. 391–400.
40. Liu, C.; Feng, M.; Dai, X.; Li, D. A New Algorithm of Backward Cloud. *J. Syst. Simul.* **2004**, *16*, 2417–2420.
41. Wu, T.; Qin, K. Image Segmentation Using Cloud Model and Data Field. *Pattern Recognit. Artif. Intell.* **2012**, *25*, 397–405.
42. Eric, R.Z. System Reliability Theory: Models, Statistical Methods, and Applications. *Technometrics* **2004**, *46*, 495–496.
43. Zhang, P.; Sun, P.; Zhang, Y.; Jiang, X. Adaptive baseline model for autonomous marine equipment and systems. *ISA Trans.* **2020**, *112*, 326–336. [CrossRef] [PubMed]
44. Cattaneo, M.E.G.V. The likelihood interpretation as the foundation of fuzzy set theory. *Int. J. Approx. Reason.* **2017**, *90*, 333–340. [CrossRef]

Disclaimer/Publisher's Note: The statements, opinions and data contained in all publications are solely those of the individual author(s) and contributor(s) and not of MDPI and/or the editor(s). MDPI and/or the editor(s) disclaim responsibility for any injury to people or property resulting from any ideas, methods, instructions or products referred to in the content.